

Electronic properties of (Ga,Mn)N thin films with high Mn content

S. Granville, B. J. Ruck, A. R. H. Preston, T. Stewart, F. Budde et al.

Citation: *J. Appl. Phys.* **104**, 103710 (2008); doi: 10.1063/1.3020536

View online: <http://dx.doi.org/10.1063/1.3020536>

View Table of Contents: <http://jap.aip.org/resource/1/JAPIAU/v104/i10>

Published by the [AIP Publishing LLC](#).

Additional information on J. Appl. Phys.

Journal Homepage: <http://jap.aip.org/>

Journal Information: http://jap.aip.org/about/about_the_journal

Top downloads: http://jap.aip.org/features/most_downloaded

Information for Authors: <http://jap.aip.org/authors>

ADVERTISEMENT



AIP Advances

Now Indexed in
Thomson Reuters
Databases

Explore AIP's open access journal:

- Rapid publication
- Article-level metrics
- Post-publication rating and commenting

Electronic properties of (Ga,Mn)N thin films with high Mn content

S. Granville,^{1,a)} B. J. Ruck,¹ A. R. H. Preston,¹ T. Stewart,¹ F. Budde,¹ H. J. Trodahl,¹ A. Bittar,² J. E. Downes,³ and M. Ridgway⁴

¹MacDiarmid Institute for Advanced Materials and Nanotechnology, School of Chemical and Physical Sciences, Victoria University of Wellington, P.O. Box 600, Wellington 6140, New Zealand

²Industrial Research Ltd., P.O. Box 31310, Lower Hutt 5040, New Zealand

³Department of Physics, Macquarie University, New South Wales 2109, Australia

⁴Department of Electronic Materials and Engineering, Australian National University, Canberra, Australia Capital Territory 0200, Australia

(Received 25 February 2008; accepted 27 September 2008; published online 19 November 2008)

Optical and dc resistivity measurements as well as x-ray spectroscopies have been performed on (Ga,Mn)N films containing Mn at up to 11 at. %. The results indicate that at higher Mn contents, the Fermi level is situated within extended states, while GaN host interband optical transitions are unaffected. The Mn state is confirmed to be $3d^5$, as in the case of lower Mn content films; however, the high Mn content merges the $3d$ levels into a band located just below the host conduction band. The Fermi level is located within these Mn states just below the conduction band, in sharp contrast to its midgap position in fully crystalline, low Mn concentration materials. The difference in the position of the Fermi level at high Mn dopant levels has important implications for the promotion of ferromagnetism in this material. © 2008 American Institute of Physics.

[DOI: 10.1063/1.3020536]

I. INTRODUCTION

The search for materials suitable for designing advanced electronic devices with multiple functionalities is one of the strongest driving factors behind materials science research. The rapidly developing field of spintronics, which combines the useful property of electronic charge with the quantum mechanical spin property, demands the development of materials that will allow practical realization of devices that are predicted to operate at reduced power consumption as compared to conventional electronic devices.¹ The ideal spintronic material will combine semiconducting and magnetic properties, and to this end III-V and II-VI dilute magnetic semiconductors such as (Ga,Mn)N (Refs. 2 and 3) and (Zn,Co)O (Refs. 4 and 5) have recently gained much attention. Reports on single crystalline films of $\text{Ga}_{1-x}\text{Mn}_x\text{N}$ with Mn concentrations up to 3 at. % ($x=0.06$) are common in the literature. However, materials containing more Mn (>5 at. %) are often reported as containing precipitates or alternate phases.⁶⁻⁹ These concentrations are above the solubility limit for substitutional Mn in GaN (Ref. 10) so that the difficulty in preparing single-phase material at higher Mn concentrations is due to the high-temperature processing needed to prepare the host III-V semiconductor GaN in highly crystalline form.

In a recent paper,¹¹ we described the preparation of strongly disordered (Ga,Mn)N films with substitutional Mn at considerably higher (up to 12 at. %, i.e., $\text{Ga}_{0.76}\text{Mn}_{0.24}\text{N}$) concentration than has been reported in fully crystalline material. This paper reports electronic property investigations of the films. The resistivity and optical properties of the films are interpreted in terms of the alterations to the electronic

states induced by the high Mn content. X-ray absorption at the Mn K and L edges has been measured to investigate the occupation state of the Mn. X-ray absorption spectroscopy (XAS) on the N and Mn K -edges delineates the conduction-band partial density of states (PDOS) and x-ray emission spectroscopy (XES) at the K -edge has been used to determine the effect of the high Mn content on the valence band PDOS.

Band structure calculations predict that dilute Mn substituting for Ga introduces Mn $3d$ orbital states into the GaN band gap.¹² The $3d$ states are crystal field split into states of e_g and t_{2g} symmetry and are further split by the on-site exchange interaction. The occupied-spin states are calculated to be approximately 1.4–1.8 eV above the valence band maximum, with the unoccupied states lying close to the conduction band edge. The occupied states are often probed with optical techniques¹³⁻¹⁵ and their position within the GaN bandgap has been found to agree with the calculated band structures for low Mn levels. It is of interest to investigate how this picture is altered at higher Mn concentrations, where the Mn ions can no longer be considered isolated.

II. EXPERIMENTAL DETAILS

(Ga,Mn)N films containing 4–11.7 at. % Mn and Mn-free nanocrystalline GaN (n_x -GaN) films were grown using ion-assisted deposition under ultrahigh vacuum conditions, as described previously.¹⁶⁻¹⁸ The films were grown to thicknesses of between 100 and 230 nm on a variety of substrates at ambient temperature. We have probed the films with a broad range of structural characterization techniques. The films are comprised of random-stacked pseudocrystals of about 5 nm diameter,^{16,17} with no sign of secondary phases or precipitates of Mn. Their chemical composition and bonding order have been established by a thorough set of charac-

^{a)}Present address: IPN, EPFL, Lausanne, Switzerland. Electronic mail simon.granville@epfl.ch.

terization studies. In particular extended x-ray absorption fine structure (EXAFS) data establish clearly that essentially all of the Mn is bonded to four neighboring N ions and that within detection limits all of the Mn is incorporated substitutionally for the Ga. Magnetization measurements at fields up to 6 T and temperatures from ambient to 2 K show no evidence of ferromagnetism; rather a Curie–Weiss analysis shows weak antiferromagnetic coupling with intercepts at -10 and -20 K, respectively, at 5 and 10 at. % Mn. dc resistivity measurements were performed from 290 to ~ 60 K on films deposited on insulating ($\rho > 10^9 \Omega \text{ cm}$) SiO_2 substrates. Optical reflection and transmission (RT) measurements were performed from 200 to 1200 nm (6.2–1.0 eV) at ambient temperature on the films deposited on the transparent SiO_2 substrates. The RT measurements were combined with thickness, as determined by Rutherford backscattering spectroscopy, to determine the optical absorption coefficients. The films' strong absorption above 3 eV required that these measurements were extended into the ultraviolet by spectroscopic ellipsometry using a Beaglehole Instruments Picometer ellipsometer.

XAS and XES were measured at the N K -edge of a (Ga,Mn)N film at room temperature using the soft x-ray undulator beamline 511 at MAXLab in Lund, Sweden, which is equipped with a spherical grating monochromator. Additionally, Mn L -edge XAS was also performed. The energy resolutions of the XES and XAS data are 0.6 and 0.1 eV, respectively. For the n_x -GaN film, XAS data were obtained at the Synchrotron Research Center, Madison, Wisconsin, and XES data obtained at the BESSY U41-PGM beamline in Berlin, Germany, and the energy scales of the two data sets matched as described previously.¹¹ Mn K -edge XAS data were measured at the Australian Synchrotron Beamline Facility at the Photon Factory in Tsukuba, Japan. Synchrotron measurements were performed in an ultrahigh vacuum environment with base pressure below 5×10^{-8} Pa, except those done in Japan, which were done at atmospheric pressure.

III. RESULTS

A. Transport and optical properties

The dc electrical resistivities of a selection of films with Mn concentrations from 4.2 to 10.8 at. % are plotted in Fig. 1. Mn-free n_x -GaN ($x=0.0$) films have an activated-type resistivity behavior with $E_A=800$ meV.¹⁸ Mn reduces the resistivity; already at 4.2 at. %, the resistivity at 290 K is $900 \Omega \text{ cm}$, four orders of magnitude lower than that of n_x -GaN, and it is reduced further to 18 and $0.08 \Omega \text{ cm}$ at 6.2 and 10.8 at. % Mn, respectively. In the films with Mn concentration below 8 at. %, the resistivity follows the variable-range hopping (VRH) form, $\rho \sim \exp[-(T_0/T)^{1/4}]$,¹⁹ establishing that the Fermi level lies in a region of localized states between the conduction and valence band mobility edges. At 10.8 at. % Mn, the temperature dependence no longer follows the VRH form, rather it is characteristic of metallic weak localization²⁰ at a Fermi energy sited in extended states.

The energy-dependent optical absorption of the (Ga,Mn)N films is plotted in Fig. 2, alongside that of

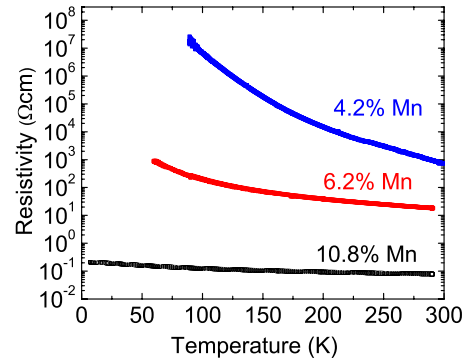


FIG. 1. (Color online) Temperature-dependent resistivity of (Ga,Mn)N films. The resistivity over the full range of measurement temperatures decreases with increasing Mn concentration. The temperature dependence changes from VRH conduction at lower Mn contents to more closely resembling weak localization at 10.8 at. % Mn.

n_x -GaN from Ref. 18. The n_x -GaN data, as have been discussed previously, show an interband edge near 3.4 eV, resembling a broadened crystalline GaN edge. The interband edge is largely retained as Mn is introduced, but there is considerable filling in of the subgap absorption below 3.4 eV. Thus, the interband transitions are largely unchanged with the addition of even high levels of Mn, but the subgap absorption rises, due largely to transitions in which either the initial or final state involves localized states within the gap. It should be noted that very recent optical transmission measurements on films with similarly high levels of substitutional Mn and larger crystallites report a similar increase in subgap absorption with increased Mn content.²¹ The Mn-induced increase of localized in-gap states probed with optical absorption is consistent with the resistivity results.

B. X-ray spectroscopies

The optical absorption and resistivity data imply that in the heavily doped samples, the Fermi level lies within a con-

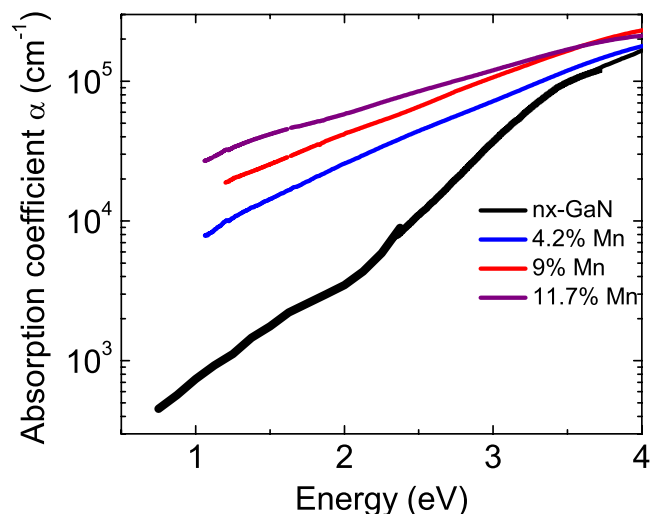


FIG. 2. (Color online) Optical absorption of (Ga,Mn)N films as a function of incident photon energy. The Mn introduces absorption below the band edge of n_x -GaN over a broad range of energies. Absorption increases as Mn content is increased, but the profile of absorption is independent of Mn concentration between 4 and 11.7 at. %.

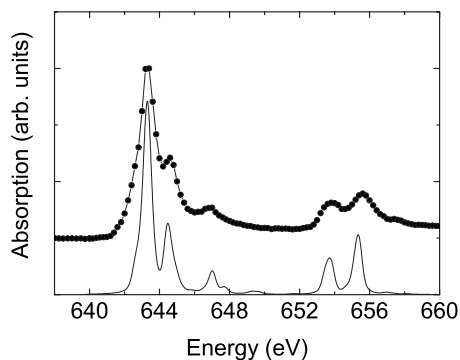


FIG. 3. Mn *L*-edge x-ray absorption spectrum in a (Ga,Mn)N film containing 11.7 at. % Mn. The spectrum features strongly resemble the signature of isolated Mn^{2+} ions. The connected points are the measured data, the line is a best-fit smoothed, simulated spectrum calculated for Mn^{2+} ions in a tetrahedral crystal field with $10Dq = -0.5$ eV. Spectra offset for clarity.

tinuum of states located in the GaN energy gap. It is thus interesting to investigate the Mn charge state in this material. Figure 3 shows XAS at the Mn *L*-edge of a film containing 11.7 at. % Mn, compared to a multiplet calculation applied to Mn^{2+} ions in the $3d^5$ configuration. The calculation was performed using the Thole code^{22,23} as described by de Groot *et al.*²⁴ The electrostatic and exchange parameters were scaled to 80% of the *ab initio* Hartree–Fock values to account for intra-atomic configuration interactions.^{24,25} A tetrahedral crystal field ($10Dq = -0.5$ eV) has symmetry consistent with Mn atoms substituting for Ga, and was also included.

The agreement between theory and experiment is excellent, showing that the majority of the Mn atoms are in the 2+ charge state. Both spectra are similar to data published by Sonoda *et al.*,²⁶ where a distinct multielectron method was used to determine an 85:15 ratio for the 2+:3+ oxidation state of Mn ions. However, in the present case, we see no evidence for any Mn^{3+} contribution at the Mn *L*-edge within the uncertainty.

The Mn^{2+} assignment is supported by XAS at the Mn *K*-edge shown in Fig. 4. We note that the position and shape of the absorption edge, with a maximum gradient at 6551.7 eV, are in agreement with the Mn absorption edge measured for substitutional Mn in single crystalline (Ga,Mn)N films

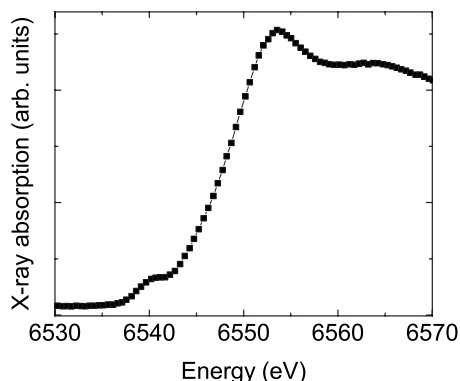


FIG. 4. X-ray absorption near-edge spectrum of Mn at the *K*-edge in (Ga,Mn)N. The position of the edge confirms a Mn^{2+} charge state. The pre-edge peak at 6541 eV indicates unoccupied Mn-related states with partial *p*-like character in the density of states.

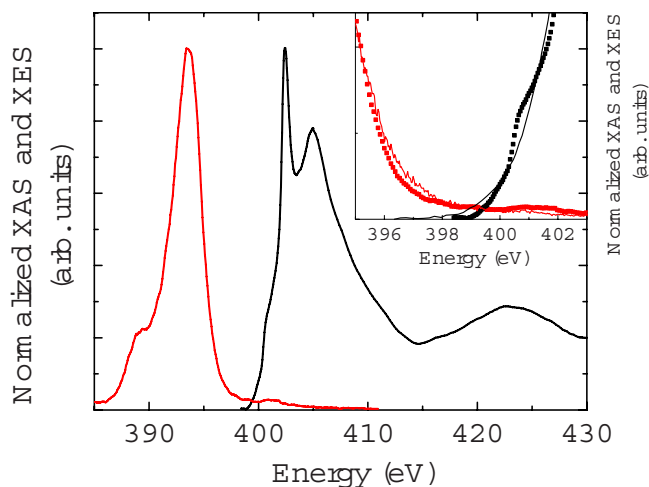


FIG. 5. (Color online) N *K*-edge x-ray absorption (black) and emission (red) spectra of (Ga,Mn)N. The emission was measured with 420 eV excitation energy. Inset: close up of the absorption and emission near the band edges (black squares), compared to *nx*-GaN (red dashed line). Note the shoulder on the absorption and the small emission peak near 401 eV, neither of which appears in the *nx*-GaN spectrum.

reported by other groups.^{27–29} The position of the edge is close to that measured in MnF_2 by Soo *et al.*,²⁸ suggesting that the incorporated Mn indeed has a $3d^5$ configuration.

The Mn *K*-edge data also show a small pre-edge feature at 6541 eV that is not seen in the Ga *K*-edge XAS. Such a peak has been interpreted as relating to unoccupied Mn $3d$ states in the GaN bandgap that have partial *p*-like character. Band structure calculations of (Ga,Mn)N assert that this *p*-like character originates from hybridization of the t_2 *d*-states with unoccupied Mn $4p$ states,^{28–30} induced by the nonspherical environment, especially the presence of the bonding N $2p$ states.^{31,32} A similar peak has been reported in (Ga,Mn)N,²⁸ where the Mn was in the 2+ charge state, while an additional lower energy peak was observed for samples containing Mn^{3+} corresponding to transitions into unfilled majority spin t_2 states.

Nitrogen *K*-edge XAS and XES results from the most heavily Mn substituted film are shown in Fig. 5, along with an inset for comparison to data from the *nx*-GaN film. These data provide a direct measure of the unoccupied and occupied N $2p$ PDOS. The level of uncertainty can be estimated by the slight noise in the *nx*-GaN XES curve in the inset. The XAS and XES of the (Ga,Mn)N film are largely similar to those from *nx*-GaN, with both resembling a broadened version of the crystalline GaN PDOS, but with an additional absorption peak centered on 402.5 eV that is related to a small concentration of molecular nitrogen trapped in the films.^{33,34} Thus, the major part of the PDOS and the gap between valence and conduction bands is retained in even this very heavily substituted film.

However, in the (Ga,Mn)N XAS spectrum, there is seen a substantial shoulder of unoccupied states merging with the conduction-band edge, which we assign to hybridization with the unoccupied Mn $3d$ states. There is also a small peak in the emission at a similar energy, corresponding to occupied Mn $3d$ states lying near the top of the band gap. Neither of these features is observed in *nx*-GaN. The small

emission peak is at an energy slightly higher than the onset in absorption, which is presumably due to the effect of the core hole, which affects only the final state of the XAS data.³⁵

The immediate implication of these data is that the Fermi level in these heavily doped (Ga,Mn)N films is located within a band of Mn states near the bottom of the conduction band. This differs from the situation expected in dilute (Ga,Mn)N samples, where calculations place the highest occupied Mn²⁺ 3*d* states at about 1.8 eV above the valence band maximum, with only unoccupied minority spin states present close to the conduction band minimum. Note that filled Mn-related states are expected to occur near the conduction band minimum in samples containing interstitial Mn (Ref. 12) but we have observed no evidence of such Mn using EXAFS,¹¹ even though the EXAFS technique is highly sensitive to such defects that significantly change the Mn local environment. The presence of a fraction of Mn in interstitial positions or at the N lattice sites cannot be completely excluded, however, the previously published EXAFS results indicate such a fraction would be small, and the dominant effect of the Mn on the XAS and XES spectra should be from the much larger proportion that substitutes for the Ga. A more likely explanation for the observed location of the Fermi level is the presence of additional defect states that codope the material. Calculations by Kulatov *et al.*³⁶ found that for Ga_xMn_{1-x}N ($x=0.03125$), in which one nitrogen atom in 32 is replaced by oxygen, the occupied Mn 3*d* states of *t*₂ character are drawn up very close to the bottom of the conduction band, while the unoccupied minority spin states are pulled fully into the conduction band. Additionally, recent calculations of the band structure with other defect states such as those arising from Ga vacancies,³⁷ clusters of Mn bonded to a common N atom³⁸ or both³⁹ provide further possibilities for the Fermi level to be placed near or at the bottom of the conduction band. We believe that our nanocrystalline (Ga,Mn)N contains compensating donor defects (e.g., unsatisfied bonds), leading to a similar effect. The study of Kulatov *et al.* also included calculations of the electronic structure for Ga_xMn_{1-x}N with *x* as high as 0.125, where the broadening of the Mn 3*d* states into a band was clearly observed. This is fully consistent with the behavior we observe in the resistivity and optical conductivity as the Mn content is increased.

IV. SUMMARY

In this work, dc resistivity and optical absorption characteristics of (Ga,Mn)N films with Mn as high as 11.7 at. % have been measured and compared with nanocrystalline GaN. Addition of Mn decreases the resistivity and the temperature dependence of resistivity of the (Ga,Mn)N with Mn ≤ 8 at. % resembles VRH conductivity. At higher Mn content, weak localization in an extended-state conduction channel dominates. Optical absorption of the films below the *nx*-GaN band edge associated with Mn states within the band gap is broad and increases with increasing Mn concentration, however, the profile of absorption does not change up to the maximum Mn content.

XAS on the Mn *L*- and *K*-edges confirm that the Mn is present in the film in the 3*d*⁵ state, suggesting Mn²⁺ ions. The shapes of the *K*-edge Mn and N XAS are in agreement with previous studies on highly crystalline (Ga,Mn)N with lower Mn concentrations, including the detection of unoccupied states at the bottom of the conduction band. In contrast to measurements on more lightly doped material, these highly Mn doped films show no occupied states near the valence band. Instead, the Fermi level in these films is located within a band of Mn states at the bottom of the conduction band. The high level of Mn incorporation in these films means the 3*d* levels merge into a band, and likely encourages higher levels of *n*-type compensating defects, which accounts for the 2+ state of the Mn.

We have presented evidence that the occupation of Mn levels in these disordered, highly Mn doped films differs significantly from that in films with lower Mn concentrations. Since the Mn 3*d* states are involved in magnetic interactions in (Ga,Mn)N, the electronic property measurements presented here have important implications for the incorporation of high levels of Mn into GaN for the promotion of high-temperature ferromagnetism, and for the effect of defects on the expected band structure.

ACKNOWLEDGMENTS

The authors gratefully acknowledge financial support from the New Zealand Foundation for Research Science and Technology through its New Economy Research Fund and through a postdoctoral fellowship of one of the authors (B.J.R.). The work of the MacDiarmid Institute is supported by a New Zealand Centre of Research Excellence award. Another author (S.G.) wishes to thank Education New Zealand for financial support of the XANES measurements. We are grateful to F. de Groot (Utrecht) for providing us with the multiplet code.

¹S. A. Wolf, D. D. Awschalom, R. A. Buhrman, J. M. Daughton, S. von Molnár, M. L. Roukes, A. Y. Chtchelkanova, and D. M. Treger, *Science* **294**, 1488 (2001).

²N. Theodoropoulou, A. F. Hebard, M. E. Overberg, C. R. Abernathy, S. J. Pearton, S. N. G. Chu, and R. G. Wilson, *Appl. Phys. Lett.* **78**, 3475 (2001).

³E. Sarigiannidou, F. Wilhelm, E. Monroy, R. M. Galera, E. Bellet-Amalric, A. Rogalev, J. Goulon, J. Cibert, and H. Mariette, *Phys. Rev. B* **74**, 041306 (2006).

⁴K. Sato and H. Katayama-Yoshida, *Physica E* **10**, 251 (2001).

⁵M. Venkatesan, C. B. Fitzgerald, J. G. Lunney, and J. M. D. Coey, *Phys. Rev. Lett.* **93**, 177206 (2004).

⁶Z. G. Hu, M. Strassburg, A. Weerakesara, N. Dietz, A. G. U. Perera, M. H. Kane, A. Asghar, and I. T. Ferguson, *Appl. Phys. Lett.* **88**, 061914 (2006).

⁷M. L. Reed, M. K. Ritums, H. H. Stadelmaier, M. J. Reed, C. A. Parker, S. M. Bedair, and N. A. El-Masry, *Mater. Lett.* **51**, 500 (2001).

⁸M. C. Park, K. S. Huh, J. M. Myoung, J. M. Lee, J. Y. Chang, K. I. Lee, S. H. Han, and W. Y. Lee, *Solid State Commun.* **124**, 11 (2002).

⁹X. Biquard, O. Proux, J. Cibert, D. Ferrand, H. Mariette, R. Giraud, and B. Barbara, *J. Supercond.* **16**, 127 (2003).

¹⁰S. J. Pearton, C. R. Abernathy, G. T. Thaler, R. Frazier, F. Ren, A. F. Hebard, Y. D. Park, D. P. Norton, W. Tang, M. Stavola, J. M. Zavada, and R. G. Wilson, *Physica B* **340–342**, 39 (2003).

¹¹S. Granville, F. Budde, B. J. Ruck, H. J. Trodahl, G. V. M. Williams, A. Bittar, M. Ryan, J. Kennedy, A. Markwitz, J. B. Metson, K. E. Prince, J. M. Cairney, and M. C. Ridgway, *J. Appl. Phys.* **100**, 084310 (2006).

¹²Z. S. Popovic, S. Satpathy, and W. C. Mitchel, *Phys. Rev. B* **70**, 161308(R) (2004).

- ¹³S. S. A. Seo, M. W. Kim, Y. S. Lee, T. W. Noh, Y. D. Park, G. T. Thaler, M. E. Overberg, C. R. Abernathy, and S. J. Pearton, *Appl. Phys. Lett.* **82**, 4749 (2003).
- ¹⁴R. Y. Korotkov, J. M. Gregie, and B. Wessels, *Physica B* **308–310**, 30 (2001).
- ¹⁵T. Graf, M. Gjukic, M. S. Brandt, M. Stutzmann, and O. Ambacher, *Appl. Phys. Lett.* **81**, 5159 (2002).
- ¹⁶F. Budde, B. J. Ruck, A. Koo, S. Granville, H. J. Trodahl, A. Bittar, G. V. M. Williams, M. J. Ariza, B. Bonnet, D. J. Jones, J. B. Metson, S. Rubanov, and P. Munroe, *J. Appl. Phys.* **98**, 063514 (2005).
- ¹⁷U. D. Lanke, A. Koo, B. J. Ruck, H. K. Lee, A. Markwitz, V. J. Kennedy, M. J. Ariza, D. J. Jones, J. Rozière, A. Bittar, and H. J. Trodahl, *Compositional and Structural Studies of Amorphous GaN Grown by Ion-Assisted Deposition*, MRS Symposia Proceedings No. 693 (Materials Research Society, Pittsburgh, 2002), p. I6.10.
- ¹⁸A. Koo, F. Budde, B. J. Ruck, H. J. Trodahl, A. Bittar, A. Preston, and A. Zeinert, *J. Appl. Phys.* **99**, 034312 (2006).
- ¹⁹D. C. Look, D. C. Reynolds, W. Kim, Ö. Aktas, A. Botchkarev, A. Salvador, and H. Morkoç, *J. Appl. Phys.* **80**, 2960 (1996).
- ²⁰E. Abrahams, P. W. Anderson, D. C. Licciardello, and T. V. Ramakrishnan, *Phys. Rev. Lett.* **42**, 673 (1979).
- ²¹D. M. G. Leite and J. H. Dias da Silva, *J. Phys.: Condens. Matter* **20**, 055001 (2008).
- ²²R. Cowan, *J. Opt. Soc. Am.* **58**, 808 (1968); R. D. Cowan, *The Theory of Atomic Structure and Spectra* (University of California Press, Berkeley, 1981).
- ²³G. van der Laan, *J. Electron Spectrosc. Relat. Phenom.* **86**, 41 (1997).
- ²⁴F. M. F. de Groot, J. C. Fuggle, B. T. Thole, and G. A. Sawatzky, *Phys. Rev. B* **42**, 5459 (1990).
- ²⁵The parameters used for Mn $3d^5$: $F_{dd}^2=8.253$ eV, $F_{dd}^4=5.131$ eV, and for Mn $2p^53d^6$: $F_{dd}^2=8.924$ eV, $F_{dd}^4=5.554$ eV, $F_{dd}^6=5.057$ eV, $G_{pd}^1=3.685$ eV, $G_{pd}^3=2.094$ eV, $\zeta_d=0.053$ eV, $\zeta_p=6.846$ eV (see Ref. 24).
- ²⁶S. Sonoda, I. Tanaka, H. Ikeno, T. Yamamoto, F. Oba, T. Araki, Y. Yamamoto, K. Suga, Y. Nanishi, Y. Akasaka, K. Kindo, and H. Hori, *J. Phys.: Condens. Matter* **18**, 4615 (2006).
- ²⁷R. Bacewicz, J. Filipowicz, S. Podsiadło, T. Szyszko, and M. Kamiński, *J. Phys. Chem. Solids* **64**, 1469 (2003).
- ²⁸Y. L. Soo, G. Kioseoglou, S. Kim, S. Huang, Y. H. Kao, S. Kuwabara, S. Owa, T. Kondo, and H. Munekata, *Appl. Phys. Lett.* **79**, 3926 (2001).
- ²⁹A. Titov, X. Biquard, D. Halley, S. Kuroda, and E. Bellet-Amalric, H. Mariette, J. Cibert, A. E. Merad, G. Merad, M. B. Kanoun, E. Kulatov, and Yu. A. Uspenskii, *Phys. Rev. B* **72**, 115209 (2005).
- ³⁰A. Titov, E. Kulatov, Yu. A. Uspenskii, X. Biquard, D. Halley, S. Kuroda, E. Bellet-Amalric, H. Mariette, and J. Cibert, *J. Magn. Magn. Mater.* **300**, 144 (2006).
- ³¹L. Kronik, M. Jain, and J. R. Chelikowsky, *Phys. Rev. B* **66**, 041203(R) (2002).
- ³²A. Filippetti, N. A. Spaldin, and S. Sanvito, *Chem. Phys.* **309**, 59 (2005).
- ³³B. J. Ruck, A. Koo, U. D. Lanke, S. Granville, H. J. Trodahl, A. Bittar, J. B. Metson, V. J. Kennedy, and A. Markwitz, *Phys. Rev. B* **70**, 235202 (2004).
- ³⁴B. J. Ruck, A. Koo, U. D. Lanke, F. Budde, H. J. Trodahl, G. V. M. Williams, A. Bittar, J. B. Metson, E. Nodwell, T. Tiedge, A. Zimina, and S. Eisebitt, *J. Appl. Phys.* **96**, 3571 (2004).
- ³⁵U. von Barth and G. Grossmann, *Phys. Rev. B* **25**, 5150 (1982).
- ³⁶E. Kulatov, H. Nakayama, H. Mariette, H. Ohta, and Yu. A. Uspenskii, *Phys. Rev. B* **66**, 045203 (2002).
- ³⁷P. Larson and S. Satpathy, *Phys. Rev. B* **76**, 245205 (2007).
- ³⁸X. Y. Cui, B. Delley, A. J. Freeman, and C. Stampfl, *Phys. Rev. B* **76**, 045201 (2007).
- ³⁹J. Kang and K. J. Chang, *J. Appl. Phys.* **102**, 083910 (2007).